Species diversity and stand structure as drivers of canopy complexity in southern African woodlands

John L. Godlee

23rd August 2021

Abstract

Atmospheric CO_2 enrichment and human-induced climate change are expected to drive woody encroachment and an increase in tree cover across African savannas, with consequences for ecosystem function, particularly related to carbon dynamics. The patch dynamics of savanna-woodland mosaics are complex however, as woody growth is mediated by seasonal fire that is itself driven by properties of the woody overtstorey. It is unclear how variation in tree species composition and stand structure in this ecosystem affects woody canopy structure, and how this might determine future vegetation dynamics. Here, I conducted a study of canopy structure in southern African savannas using terrestrial LiDAR, at sites in Bicuar National Park, Angola and Mtarure Forest Reserve, Tanzania, to explore relationships between tree species diversity, species composition, canopy structure, and the spatial distribution of trees. I found consistent weak positive effects of species diversity on plot scale canopy complexity. Species diversity caused an increase in canopy height, canopy closure, and within-canopy structural complexity. However, stochasticity in neighbourhood scale woody structure masked species diversity effects at small spatial scales. Finally I found that spatial clustering of trees in space led to a reduction in canopy closure, even within clustered areas, suggesting that disturbance by fire and herbivory not only reduce canopy cover at the landscape scale, but also reduce canopy cover at smaller spatial scales **But how does disturbance lead to clustering? Could just say "suggesting"**

1 Introduction

Atmospheric CO_2 enrichment, coupled with climate change and changing disturbance regimes, is expected to drive woody encroachment, i.e. proliferation of trees in previously non-wooded areas, and increased growth of trees in currently wooded areas, across the savanna biome over the coming century (Criado et al., 2020; Mitchard & Flintrop, 2013; Stevens et al., 2016). As atmospheric CO_2 concentrations increase, C_3 trees are expected to gain a competitive edge over C_4 grasses due to differences in photosynthetic pathway and carbon use efficiency (Buitenwerf et al., 2012), with cascading effects on canopy cover, grass growth, and disturbance regime (Bond & Midgley, 2012). If realised, woody encroachment and woody densification will have significant effects on the global carbon cycle, as more CO_2 is stored in woody biomass, as well as myriad other effects on ecosystem structure (Donohue et al., 2013). Indeed, tropical savannas have been identified as the fastest increasing component of the terrestrial carbon sink (Sitch et al., 2015). Previous studies however, have reported wide variation in rates of woody encroachment and densification (Mitchard & Flintrop, 2013), particularly in disturbance-prone savannas such as miombo woodlands in southern Africa (Axelsson & Hanan, 2018), and it is unclear how the fertilisation effect of atmospheric CO_2 enrichment will interact with other ecosystem properties to alter vegetation structure (Körner, 2017; Reich et al., 2014).

Savanna vegetation is defined by the coexistence of trees and grasses (Scholes & Archer, 1997). In the tropical mesic savannas of southern Africa, disturbance by fire and herbivory are the main limitations on tree cover, preventing the competitive exclusion of shade-sensitive C_4 grasses where climatic conditions would otherwise allow for closed canopy forest (Sankaran et al., 2005). C_4 grasses also provide the main fuel source for seasonal fires in these savannas (Frost, 1996),

producing a positive feedback where an increase in tree cover reduces grass fuel load, reducing fire frequency and intensity, increasing tree cover, and so on (Staver & Koerner, 2015). As such, even small perturbations in tree cover can lead to large changes in vegetation structure if critical thresholds of tree cover are crossed (Hirota et al., 2011). Previous research has sought to identify environmental factors which affect tree cover and its responses to atmospheric CO_2 enrichment, but few have considered the functional role of the existing tree community and its effect on ecosystem processes.

Canopy structure describes the spatial distribution and density of tree canopy foliage (Lowman & Rinker, 2004). Canopy structural complexity, i.e. the spatial heterogeneity of foliage distribution within the canopy, has been linked to increased net ecosystem productivity (Baldocchi & Wilson, 2001; Chen et al., 2012; Gough et al., 2019; Hardiman et al., 2011; Law et al., 2001; Morin, 2015), increased resilience of productivity (Pretzsch, 2014), reduced understorey light penetration (Fotis et al., 2018; Scheuermann et al., 2018), and greater moderation of understorey micro-climate (Wright et al., 2017). Furthermore, in temperate and boreal forests, functional differences among coexisting tree species in their vertical and horizontal canopy occupation provides a link between species diversity, canopy structural complexity and canopy density, with canopy complexity constituting a mechanism for observed positive biodiversity-ecosystem function effects in wooded ecosystems (Barry et al., 2019; Pretzsch, 2014). In tropical savannas, tree species diversity might therefore influence ecosystem-level woody thickening in response to elevated atmospheric CO_2, where competition effects in diverse tree communities are reducted due to niche separation, and can more effectively increase foliage density and reduce understorey light penetration, excluding grass and thus reducing the probability of disturbance.

As well as the species diversity of trees, the spatial distribution and relative size of tree stems, i.e. stand structure, is also expected to affect canopy structural complexity (Stark et al., 2015). Heterogeneity in stem size, whether a result of species diversity, disturbance history or some other factor, is expected to increase canopy complexity and canopy density as individuals of different sizes occupy different parts of the vertical canopy space (Panzou et al., 2020), and may differ in light requirements (Charles-Dominique et al., 2018). Additionally, clustering of individuals in space is expected to increase canopy structural heterogeneity across the wider savanna landscape, but ultimately decrease total foliage density due to an increase in competitive interactions (Dohn et al., 2017). Clustering may occur as a result of disturbance history, facilitation effects among individuals in stressful environments (Ratcliffe et al., 2017), or due to other limitations on establishment arising from growth strategy (). More diverse communities may allow greater stem density and greater foliage density, as differences in canopy occupancy among species reduce negative effects competition among individuals on growth (Gough et al., 2019).

Functional differences among floristic types of savanna may also drive variation in canopy complexity, irrespective of species diversity. Some savanna trees form denser canopies than others, as a result of variation in leaf size and branch architecture. Previous studies have compared the branch architecture of ex-Acacia (e.g. *Senegalia* and *Vachellia* spp.) and miombo (e.g. *Julberardia*, *Brachystegia*, and *Isoberlinia*) archetypal tree species. While ex-Acacia species tend to inhabit drier, heavily grazed areas, miombo species tend to inhabit dystrophic wetter areas structured heavily by fire (Ribeiro et al., 2020). These studies have shown that ex-Acacia species develop sparser canopies, cagey branch architecture, and wider spreading crowns, while dominant Fabaceae species from the miombo develop thicker, taller canopies, and can grow to large trees (Archibald & Bond, 2003; Mugasha et al., 2013; Privette et al., 2004). Similarly, dominant miombo Fabaceae species from the Detarioideae subfamily have been shown to exhibit wider crowns and grow taller than coexisting species from the Combretaceae family (). Shenkin et al. (2020) showed that Fabaceae tree species from tropical forests exhibit wider and more voluminous tree crowns than other common families of tropical trees. Under identical stem densities, miombo woodland species may therefore exclude grass more effectively than ex-Acacia

or Combretaceae species given these differences in growth form.

Canopy complexity is multi-dimensional and has previously been explained using a plethora of simple metrics that originated in forest and community ecology (Kershaw et al., 2017). Assessments of canopy complexity have most often modelled tree canopies as a series of ellipses (2D), ellipsoids or cones (3D) based on field measurements with measuring tapes (Jucker et al., 2015), or used surrogate proxies for 3D canopy structure, due to its inherent complexity (Seidel et al., 2011). Measurements of this kind are time consuming and yet remain an over-simplification of canopy structure. Alternatively, canopy closure is often measured using indirect optical methods which partition sky from canopy material, i.e. with hemispherical photography or the commonly used LAI-2000, providing a 2D representation of the canopy but lacking information on vertical canopy structure (Jonckheere et al., 2004). In recent years, particularly in temperate and boreal forests, LiDAR (Light Detection And Ranging) has emerged as a suitable technology for rapidly and precisely assessing canopy structure in 3D, conserving information on 3D structure of the calibre that is required to understand it's complexities (Calders et al., 2020; Muir et al., 2018). In tropical savannas, very few studies have used terrestrial LiDAR for vegetation analyses, and in southern Africa all existing studies have been located at the Skukuza Flux Tower in Kruger National Park, South Africa (Muumbe et al., 2021). Pioneering work describing the ecology of southern African savannas placed large emphasis on canopy structural diversity as a mediator of ecosystem function (Solbrig et al., 1996), but much of that understanding of savanna vegetation structure was derived from traditional mensuration methods. Using terrestrial LiDAR to measure canopy complexity in southern African savannas therefore offers a unique chance to validate accepted theory and describe differences in ecosystem structure among savanna vegetation types in finer detail than previously possible.

In this study I applied terrestrial LiDAR techniques to woodland-savanna mosaics at two sites in southern Africa, with the aim of increasing understanding of how various measures of tree canopy complexity relate to tree diversity and stand structure. I hypothesise that tree neighbourhoods with greater tree species diversity, and greater heterogeneity in stem size may allow greater canopy complexity and foliage density. Thus, more diverse savannas might exhibit a higher potential woody biomass, and more effectively increase their growth under elevated atmospheric CO_2, promoting woody thickening. I also consider the functional differences in canopy architecture among tree communities and how this affects canopy closure and total canopy occupancy.

2 Materials and methods

2.1 Study sites

Field measurements were conducted at two sites, Bicuar National Park, in southwest Angola (S15.1°, E14.8°), and Mtarure Forest Reserve, in southeast Tanzania (S9.0°, E39.0°) (Figure 1). At each site, 1 ha (100×100 m) plots were located in areas of savanna-woodland vegetation, across a gradient of stem density and a range of savanna floristic archetypes. In Angola, 15 plots were sampled, while in Tanzania, seven were sampled following the curtailment of fieldwork due to COVID-19 travel restrictions. Fieldwork was conducted between February and April at both sites, during the peak growth period of each site in order to capture the maximum foliage volume in the canopy.

2.2 Field measurements

Within each 1 ha plot, each woody stem $\geq$ 5 cm stem diameter was identified to species, the stem Diameter at Breast Height (DBH) was measured at 1.3 m above the ground, and the stem

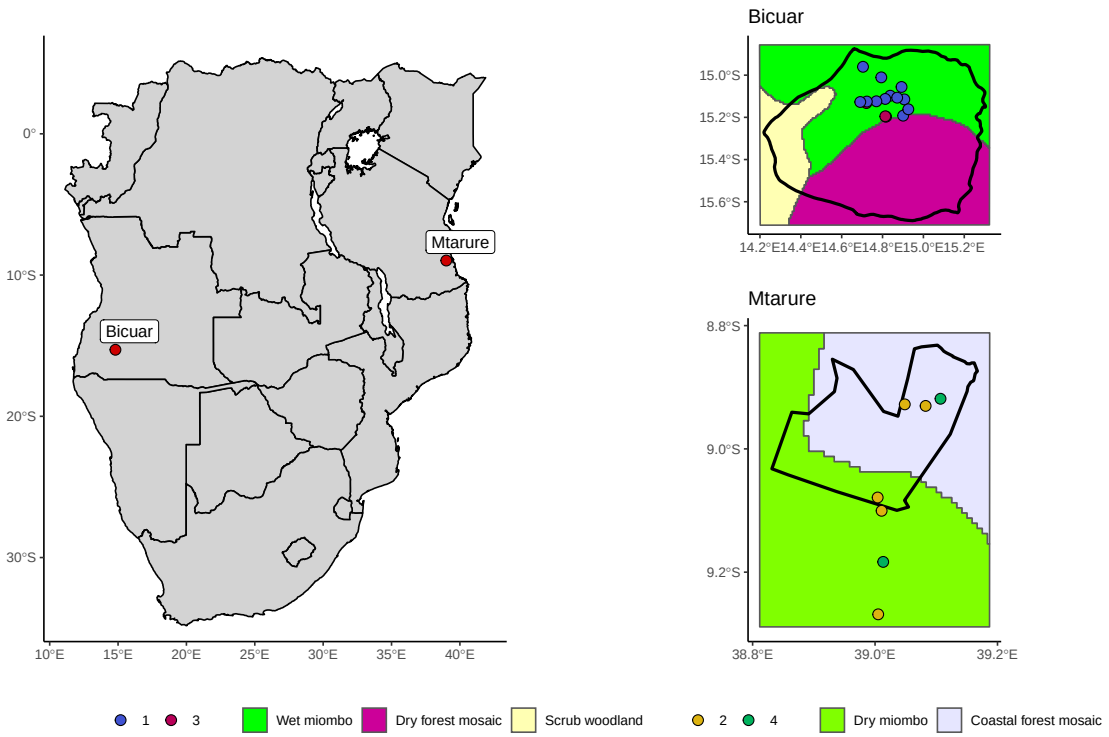

Figure 1: Location of study sites within southern Africa (left), and of 1 ha plots within each site (right). The black outlines in each site map denote the boundaries of protected areas which encompass the majority of study sites, Bicuar National Park in Angola (top), and Mtarure Forest Reserve in Tanzania (bottom). The background of each site map is a re-classified version of White's vegetation map (White, 1983). Points in site maps are shaded according to vegetation type identified by hierarchical clustering of tree genera abundances. Note that all maps are on different scales.

location within the plot was recorded using tape measures. Each 1 ha plot was sampled by nine 10 m diameter circular subplots arranged in a regular grid, with a 15 m buffer from the plot edge and 35 m between subplots. For each subplot, the distance and direction from the subplot centre of each stem >5 cm diameter with canopy material inside the subplot was recorded. Within each subplot, a variable number of scans were recorded using a Leica HDS6100 phase-shift Terrestrial Laser Scanner (TLS). The number and position of scans within a subplot was determined by the arrangement of canopy material in the subplot, to minimise shadows within the canopy of the subplot, and to maximise canopy penetration. The number of scans per subplot ranged between one and five across both sites. Extended field methods and data analysis methods are described in Chapter 6.

2.3 Data analysis

2.3.1 TLS processing

Point clouds from scans in each subplot were registered and unified using Leica Cyclone (version 9.1), using five reflective cross targets visible to all scans as anchor points. Point clouds were voxelised to cubic voxels of different sizes depending on the application of the data. Subplot height profile estimation and gap fraction was conducted using 5 cm^3 voxels, while whole plot canopy rugosity was estimated using 50 cm^3 voxels. Voxels were classified as 'filled' if they intersected one or more points. Variation in voxel size reflects the spatial scale of each analysis, and is bounded by the beam divergence of the scanner over longer distances (Cifuentes et al., 2014). Choosing voxels that are too small can result in pock-marked representations of surfaces that are especially problematic when calculating larger scale canopy complexity metrics such as canopy top roughness, while voxels that are too large can result in an over-estimation of plant volume when estimating canopy foliage density at the subplot scale (Cifuentes et al., 2014; Seidel et al., 2012).

The noise reduction algorithm from Rusu et al. (2008) was used to discard points based on mean nearest neighbour distances, with a mean number of neighbours of eight, and a standard deviation threshold of 1.96. This effectively removed 'ghost points' produced by partial beam interceptions and also removed many erroneous returns caused by airborne dust particles, which was common at these study sites. Raw points clouds for each subplot had a mean of ~2.9e+08 points, ~4.5e+07 points after voxelisation to 5 cm^3, and ~2.1e+07 points after noise reduction.

Ground points were classified using the Progressive Morphological Filter (PMF) from Zhang et al. (2003). Point cloud height was reclassified based on this revised ground layer by measuring the vertical distance between the nearest ground point and each point. Points below 1.3 m height above ground were discarded for calculations of foliage density, canopy cover, and canopy complexity, as points below this threshold where often occupied by long grass.

2.3.2 Canopy complexity metrics

Ray-tracing was used to estimate canopy closure in each subplot, i.e. the proportion of the sky hemisphere occluded by plant material at the subplot centre from multiple TLS scans. Hemispherical images were created using the POV-Ray ray-tracing software (Persistence of Vision Pty. Ltd., 2004). Filled voxels were represented as black cubes filling the voxel volume, with a white sky box and no light source. A 'camera' with a 180° fisheye lens was placed at the subplot centre within POV-Ray, at a height of 1.8 m pointing directly upwards. The images produced by POV-Ray were analysed using Hemiphot (ter Steege, 2018) to estimate canopy closure. Canopy closure estimates from the TLS were validated with hemispherical photographs taken at the same location and processed using the same method in Hemiphot, and compared

using Pearson's correlation ($r(195)$=0.87, p<0.001). A plot level estimate of canopy closure was calculated as the mean of subplot canopy closure measurements.

Effective Number of Layers (ENL) was calculated according to Ehbrecht et al. (2016) to measure vertical variation in subplot foliage density. ENL is calculated as the exponential Shannon index (i.e. the Hill number of order $q = 1$) of foliage density among 50 cm vertical layers within each subplot:

$$\mathrm{ENL} = \exp\Big(-\sum_{i=1}^{N} p_i \times \ln p_i \Big) \tag{1}$$

Where p_i is the proportion of filled voxels in the 50 cm layer i, and N is the total number of layers.

Total foliage density was calculated within each subplot as the area under the curve of the foliage height profile. Total foliage density was also calculated at the plot level as the sum of filled 50 cm^3 voxels across the plot.

Plot level canopy surface models were extracted using the 99th percentile of canopy height in 10 cm^2 columns. A pit-filling algorithm provided by Khosravipour et al. (2014) was applied at 50 cm^2 resolution to reduce the effects of incomplete canopy penetration in dense canopies. Whole plot canopy complexity was measured by two metrics. Canopy top roughness was measured as the coefficient of variation of canopy height across the plot. Canopy rugosity was measured according to Hardiman et al. (2011), as the coefficient of variation of vertical and horizontal foliage density within 0.5 m^3 cubic bins.

2.3.3 Stand structure

For each subplot, an adapted version of the Iterative Hegyi index was used to estimate crowding, as an alternative to stem density which does not adequately capture crowding at small spatial scales when only a small number of trees are included in the sample (Hegyi, 1974). The coefficient of variation of stem diameter was calculated as a measure of the heterogeneity of tree size in the neighbourhood.

At the plot level, the regularity of species spatial distribution was estimated using the spatial mingling index (von Gadow & Hui, 2002), which scores each tree based on whether it shares species identity with its nearest neighbours. The spatial regularity of trees was estimated using the uniform angle index (winkelmass) (von Gadow & Hui, 2002), which scores each tree based on the angles between nearest neighbours. Additionally, the degree of spatial clustering of trees was measured using Voronoi tessellation, as the coefficient of variation of Voronoi cell areas (Ong et al., 2012). Finally, plot level tree density was calculated to estimate crowding at the plot scale. See Chapter 6 for more information on the behaviour of the spatial mingling index and uniform angle index.

2.3.4 Statistical analysis

Non-metric Multi-dimensional Scaling (NMDS) was used to describe variation in species composition among plots, using genus-level basal area weighted abundance in each plot. Stems that could not be identified to genus were excluded from this analysis, which accounted for 0.2% of the total basal area recorded. Four distinct vegetation types, two from each site (Table 1), were identified using hirerarchical clustering of the four dominant NMDS ordination axes. Clusters were further described using Dufrêne-Legendre indicator species analysis and by ranking tree species according to abundance across all plots within each cluster.

Table 1: Description of the vegetation type clusters, identified using the Ward algorithm based on basal area weighted genus abundance. AGB = Above-Ground woody Biomass. Species richness, stem density and AGB are reported as the median among plots, with the interquartile range in parentheses.

Site	Cluster	N sites	Richness	Stem density (Stems ha^{-1})	AGB (t ha^{-1})
Bicuar	1	12	17(2)	642(194)	41(8.4)
Mtarure	2	5	23(4)	411(137)	72(11.9)
Bicuar	3	3	6(1)	196(55)	77(7.3)
Mtarure	4	2	12(2)	288(73)	9(0.2)

Species diversity at both the subplot and plot level was measured using the exponential Shannon index (i.e. the Hill number of order $q = 1$), calculated using tree species abundance.

Linear mixed effects models tested the effects of tree species diversity and stand structural diversity on subplot canopy complexity metrics. Mixed models used a nested random intercept structure to account for the sampling design of subplots within plots and plots within vegetation types. Separate models were fitted for each canopy complexity metric, resulting in four models at the subplot level. Effect sizes among fixed effects in maximal models were compared for each canopy complexity metric, using the 95% confidence interval of the effect size to ascertain whether a fixed effect was significant by whether the confidence interval overlapped zero (Nakagawa & Cuthill, 2007). AIC values and Akaike weights of models with different combinations of fixed effects were compared to determine which combination of diversity and structural metrics best explained variation in each canopy complexity metric.

Path analysis was used to test whether tree species diversity may influence canopy complexity indirectly through its effect on stand structure, using the `piecewiseSEM` R package (Lefcheck, 2016). The path analysis investigated the direct effect of plot species diversity on mean plot canopy closure, as well as the indirect effect of diversity on canopy closure via the coefficient of variation of basal area, with random intercept terms for each vegetation type. The ex-Acacia vegetation type was represented by only two plots and could not be included in this model due to lack of replication.

Statistical analysis of the determinants of plot level canopy complexity metrics were conducted using linear models. Again, these models excluded the ex-Acacia vegetation type due to lack of replication. As with the subplot linear mixed models, predictor variable effect sizes were used to assess predictor variable significance, and comparison of candidate models using AIC, Akaike weights, and model R^2 values was used to determine which combination of predictors best explained each canopy complexity metric.

3 Results

3.1 Description of vegetation types

Indicator species analysis shows that the four identified vegetation types constitute common southern African savanna floristic archetypes (Table 2). Cluster 1, found in Bicuar National Park contains typical miombo species from the Detarioideae subfamily, such as *Julbernardia paniculata*. Cluster 1 is the most frequent vegetation type in this study, with 12 plots. Cluster 1 has the highest stem density, but lower AGB than Clusters 2 or 3, which contain larger individuals with disproportionately higher biomass. Cluster 2, found in Mtarure Forest Reserve, is dominated

Table 2: Floristic description of the vegetation type clusters. Dominant species are the most abundant individuals across all plots per cluster. Indicator species are derived from Dufrêne-Legendre indicator species analysis with the three highest indicator values.

Cluster	Dominant species	Indicator species	Indicator value
1	Julbernardia paniculata	Strychnos spinosa	0.83
	Burkea africana	Combretum collinum	0.74
	Combretum collinum	Julbernardia paniculata	0.70
2	Diplorhynchus condylocarpon	Pteleopsis myrtifolia	1.00
	Pseudolachnostylis maprouneifolia	Diplorhynchus condylocarpon	0.89
	Gymnosporia senegalensis	Pseudolachnostylis maprouneifolia	0.81
3	Baikiaea plurijuga	Baikiaea plurijuga	0.94
	Baphia massaiensis	Baphia massaiensis	0.83
	Philenoptera nelsii	Philenoptera nelsii	0.45
4	Combretum apiculatum	Vachellia nilotica	0.99
	Burkea africana	Combretum apiculatum	0.70
	Bauhinia petersiana	Senegalia polyacantha	0.62

by *Pteleopsis myrtifolia*, a common miombo species from the Combretaceae family. Indeed, Cluster 2 also contained other common miombo species shared with plots in Cluster 1, such as *Julbernardia globiflora* and *Pseudolachnostylis maprouneifolia*, but these clusters remain distinct due to biogeographic variation in endemic genera at the longitudinal extremes of the miombo ecoregion represented by the two sites in this study. Cluster 3 represents *Baikiaea* woodland, found on Kalahari sands in southern Angola. It is species poor and dominated by *Baikiaea plurijuga* which forms large spreading canopy trees with high AGB. Other shrubby species that coppice readily in response to disturbance by fire such as *Baphia massaiensis* are also common. Cluster 4, found in Mtarure is a type of ex-Acacia woodland, dominated by *Vachellia* and *Senegalia* spp. This vegetation type was not well represented in the study, with only two plots, precluding its use in some multi-level statistical analyses due to lack of replication. Cluster 4 had far lower AGB than the other clusters (Table 1).

Differences in canopy structure among the four vegetation types are evident through observation of canopy surface models for typical plots within each vegetation type (Figure 4), and by comparing canopy complexity metrics (Figure 5). Cluster 1 shows many overlapping crowns forming a nearly contiguous canopy surface, and the heighest plot foliage density of all clusters. Though most trees in Cluster 1 have smaller crowns than those in Cluster 2, which also forms a nearly contiguous canopy. The largest trees in Cluster 2 grow taller and have a wider spreading canopy than those in other vegetation types. Cluster 3 shows two distinct size classes of tree, the large *Baikiaea plurijuga* forming clear isolated canopies, and much smaller scattered shrubby individuals in the understorey. Cluster 4 shows many small shrubby individuals with irregular canopy shapes, but a greater total crown area coverage than Cluster 3.

3.2 Bivariate relationships

Bivariate plots and linear models show that subplot species diversity, measured as the true-numbers equivalent of the Shannon diversity index of the tree neighbourhood around each 10 m diameter subplot, appears to have weak positive effects on subplot canopy layer diversity (β=1$\pm$0.27, F(2,180)=17, p<0.001, R^2=0.09), canopy closure (β=0.05$\pm$0.017, F(2,181)=7.3,

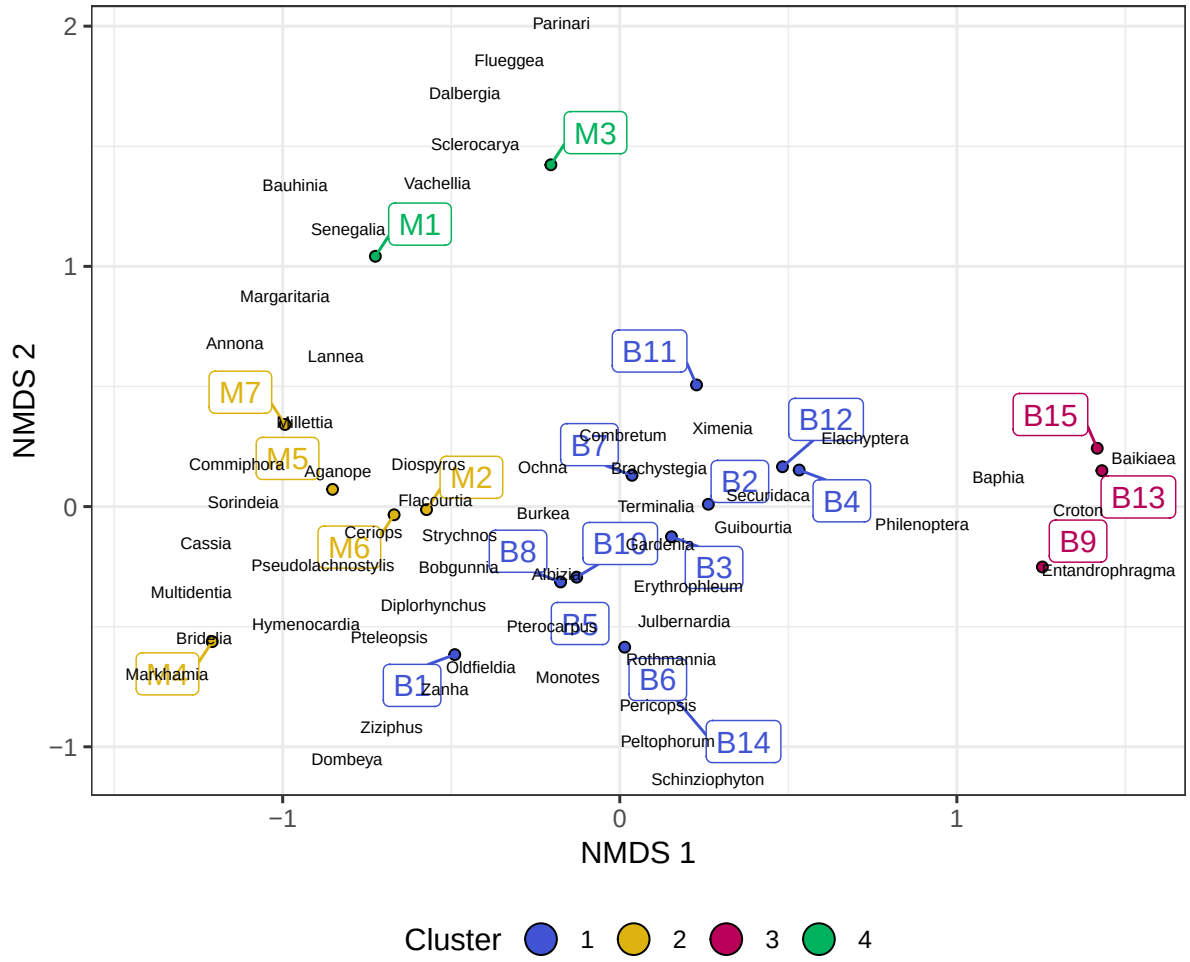

Figure 2: The first two axes of a Non-metric Multi-Dimensional Scaling (NMDS) analysis of tree genus diversity in each plot. Genus scores are labelled as black text, while plot scores are labelled as coloured points. Plots are shaded by vegetation types identified by hierarchical clustering: 1) B1-B8, B10-B12, B14, dominated by core miombo species such as *Julbernardia* spp., *Brachystegia* spp.; 2) M2, M5, M6, and M7, also dominated by core miombo genera with some genera not found in Bicuar National Park such as *Commiphora* and *Sorindeia*; 3) B9, B13 and B15, dominated by *Baikiaea plurijuga*; and 4) M1, M3, and M4, dominated by *Senegalia* spp., *Vachellia* spp., and *Combretum* spp.

$p<0.01$, $R^2=0.04$) and foliage density (β=3163±1063, F(2,180)=8.9, $p<0.01$, $R^2=0.05$) (Figure 3). The Hegyi crowding index had strong positive effects on all canopy complexity metrics, as expected. The effect of Hegyi crowding on subplot canopy complexity metrics was similar across all vegetation types. Structural diversity, measured as the coefficient of variation of subplot stem basal area had significant weak positive effects on total canopy foliage (β=87±30, F(2,167)=8.6, $p<0.01$, $R^2=0.05$), layer diversity (β=0.03±0.0076, F(2,167)=18, $p<0.001$, $R^2=0.1$), and canopy closure (β=0.001±0.00048, F(2,168)=6.3, $p<0.05$, $R^2=0.04$).

At the plot level, effects of species diversity and stand structure on canopy complexity were similarly weak (Figure 3). The effect of spatial regularity of stems on canopy closure, measured by uniform angle index, was clearly negative (β=-3±1.7, F(2,20)=3.9, p=0.06, $R^2=0.2$), while the effect of spatial clustering of stems, measured by the coefficient of variation of Voronoi cell area, was negligible (β=0.002±0.0058, F(2,20)=0.17, p=0.69, $R^2=0.008$). Additionally, there was a non-significant negative effect of the coefficient of variation of basal area on whole canopy rugosity (β=-1±0.53, F(2,16)=3.7, p=0.07, $R^2=0.2$). As expected, tree density had strong positive effects on foliage density, canopy height and canopy closure, and negative effects on canopy roughness and canopy rugosity. Species diversity appeared to have strong positive relationships with canopy closure (β=0.01±0.012, F(2,20)=0.74, p=0.4, $R^2=0.04$) and canopy height (β=0.3±0.13, F(2,16)=6, $p<0.05$, $R^2=0.3$), and negative effects on canopy roughness (β=-2±0.95, F(2,16)=4, p=0.06, $R^2=0.2$) and canopy rugosity (β=-13±12, F(2,16)=1.2, p=0.28, $R^2=0.07$). Linear models were highly leveraged by one particularly speciose plot in Cluster 2, with over 40 species, though when this plot was removed, linear model slopes remained significant and with the same sign. Additionally, Cluster 4 represented an outlier in plot level bivariate relationships, with low canopy closure, low canopy height, low species diversity, and low variation in stem size.

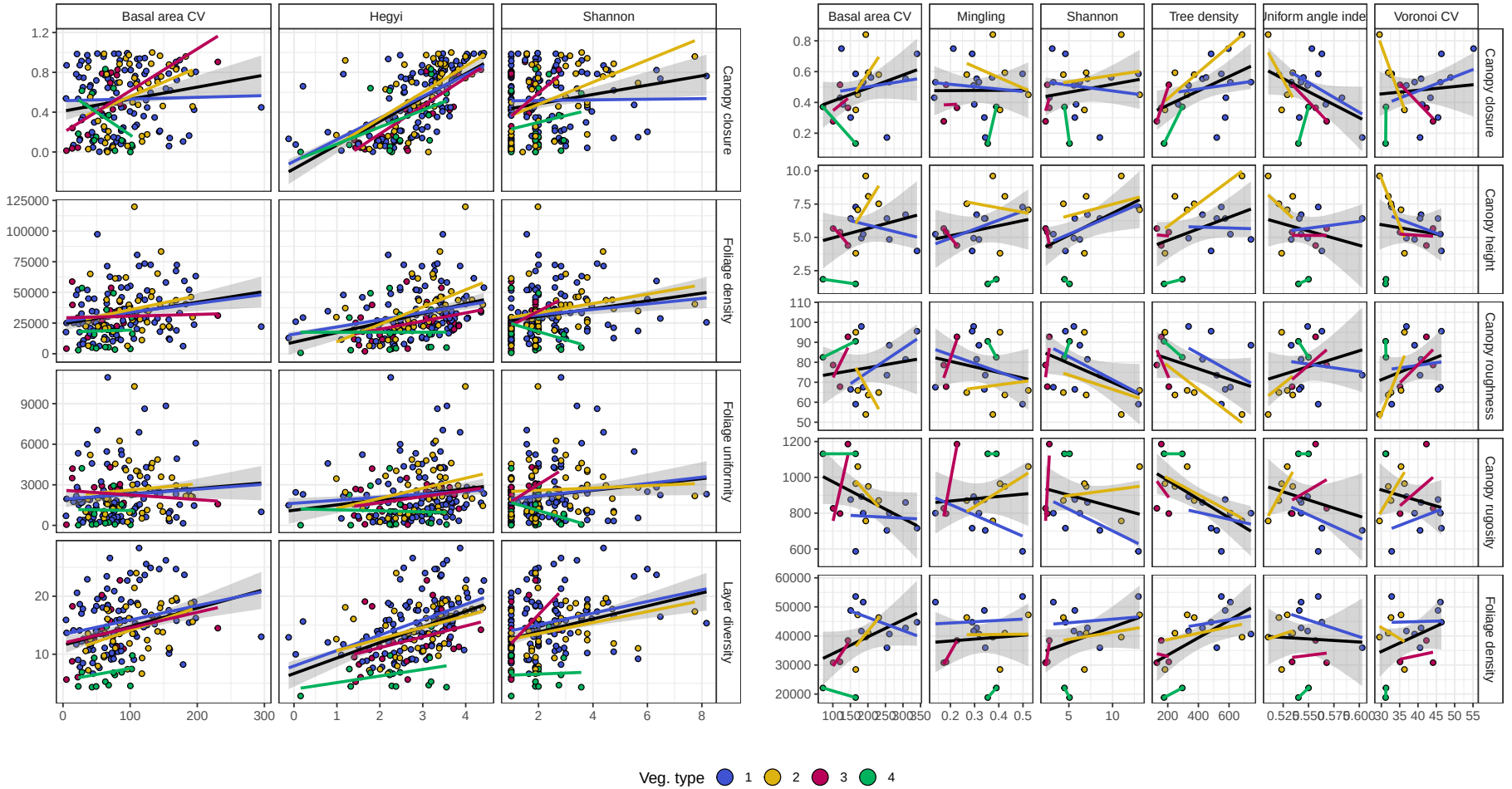

Figure 3: Bivariate relationships between diversity/stand structure metrics (x axis) and canopy complexity metrics (y axis), at both the subplot level (left) and the plot level (right). Points and linear model lines of best fit are coloured by vegetation type. Black lines of best fit are linear models including all plots, with a 95% confidence interval. See **??** for a comparison of linear model fits by vegetation type.

3.3 Subplot mixed models

Linear mixed effects models showed that species diversity of the subplot neighbourhood had negligible and poorly constrained effects on canopy complexity (Figure 6). As seen in the subplot bivariate relationships Figure 3, the Hegyi crowding index had strong positive effects on all measured canopy complexity metrics, though these effects were non-significant for vegetation clusters 3 and 4. Heterogeneity of stem basal area had a significant positive effect on layer diversity, but there was wide variation in vegetation type marginal effects for Clusters 3 and 4, due to low levels of replication. Cluster 3 had a significant positive effect of species diversity on foliage distribution uniformity, while none of the other vegetation clusters did.

Model selection showed that none of the best models for subplot canopy complexity metrics included species diversity (Table 4). The coefficient of variation of basal area was included in the best models for layer diversity and foliage density, with the fixed effects for these models explaining 50% and 27% of the variation in these metrics, respectively. The random effects of vegetation type and plot identity described most of the variation in layer diversity and foliage density. All models were better than random effects only models according to AIC values.

3.4 Whole-plot multivariate linear models

While species diversity had varying effects on different plot level canopy complexity metrics, the confidence intervals on these effect sizes were wide (Figure 7). Species diversity had a significant positive effect on canopy height (β=3$\pm$0.96, p<0.05), a non-significant positive effect on canopy closure (β=0.07$\pm$0.085, p=0.41), but a negative effect on canopy surface roughness (β=-13$\pm$6.8, p=0.09). Plot tree density had negligible effects on canopy complexity, except for canopy rugosity (β=-61$\pm$42, p=0.17), in contrast to the effect of Hegyi crowding on subplot canopy complexity. Structural diversity, measured by the coefficient of variation of basal area had a positive effect on canopy roughness (β=5$\pm$3.4, p=0.18). Spatially explicit measures of structural and species diversity, measured by the uniform angle index and spatial mingling index respectively, had negligible effects on all canopy complexity metrics. One exception was the effect of uniform angle index, i.e. the spatial clustering of stems, on canopy closure, which was clearly negative (β=-0.08$\pm$0.043, p=0.1).

Despite the weak effect sizes of species diverity on canopy complexity at the plot level, model selection showed that canopy height, canopy roughness, and canopy closure were better explained by models which included species diversity (Table 5). Additionally, the best model for canopy closure included spatial clustering of trees. Though the model for canopy roughness was only marginally better than a null model, and had a non-significant p-value. Canopy rugosity was poorly predicted by all candidate models.

3.5 Path analysis

The path analysis investigating the indirect effect of subplot species diversity on canopy closure via the coefficient of variation of basal area showed that while species diversity had a strong positive significant effect on basal area variation, the effect of basal area variation on canopy closure remained negligible (Figure 8). The indirect effect of species diversity on canopy closure via basal area coefficient of variation was -5e-04, while the direct effect was -0.078. As in the bivariate relationships and plot level linear models, species diversity had a weak positive significant effect on canopy closure, while the major driver of canopy closure was the Hegyi crowding index.

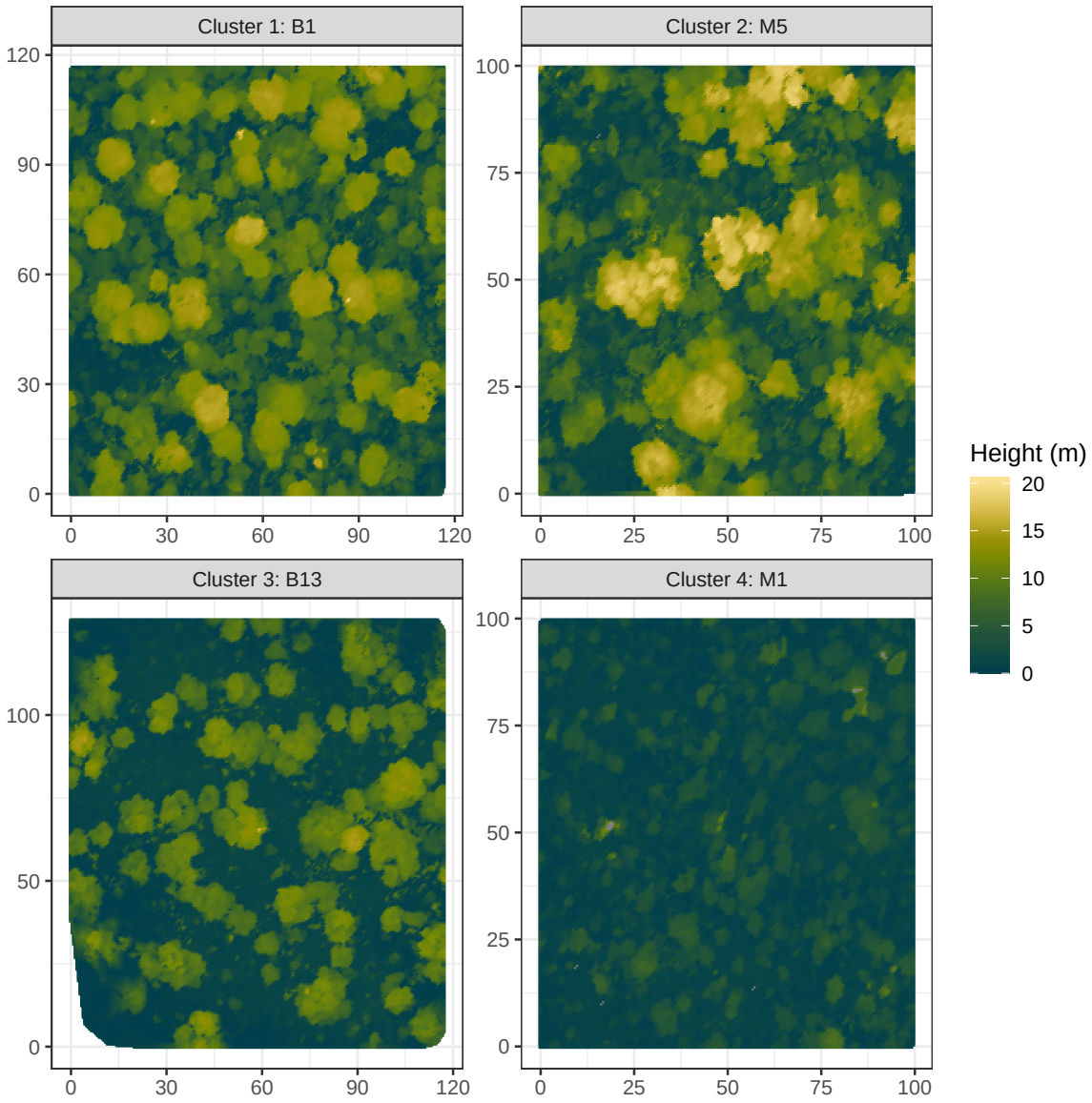

Figure 4: Representative canopy surface models for each vegetation type identified in the Non-metric Multi-dimensional Scaling (NMDS) clustering analysis. Panel titles show the plot name and the vegetation type.

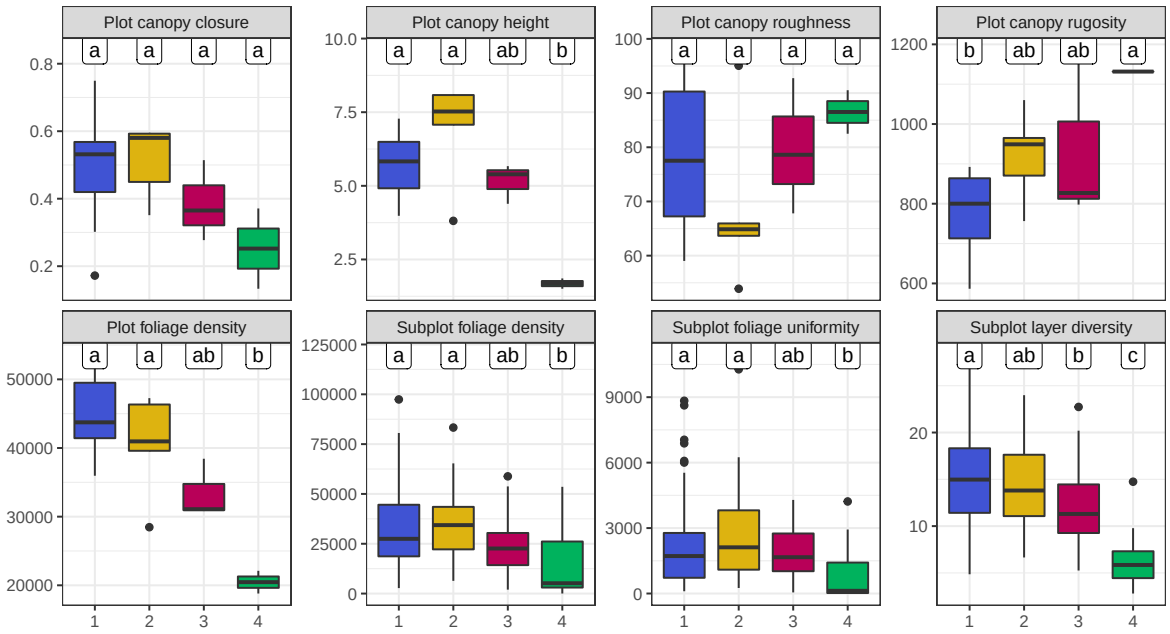

Figure 5: Box plots showing variation in canopy complexity metrics among the four vegetation types identified in the Non-metric Multi-dimensional Scaling (NMDS) clustering analysis. Thick lines show the median, boxes show the interquartile range (IQR), whiskers show 1.5×IQR, and points show outliers beyond these limits. Labels above each box plot group vegetation types according to significant differences in pairwise Tukey's tests; vegetation types sharing a letter are not significantly different.

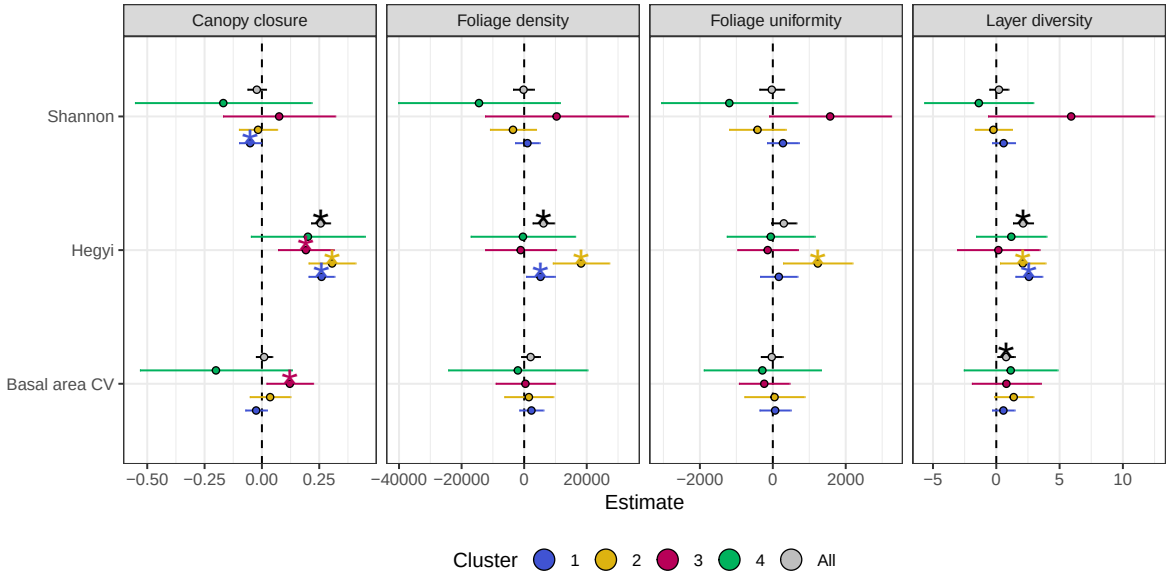

Figure 6: Standardised fixed effect slopes for each model of a canopy complexity metric. Slope estimates where the interval (±1 standard error) does not overlap zero are considered to be significant effects, marked with asterisks. Points are coloured according to vegetation type.

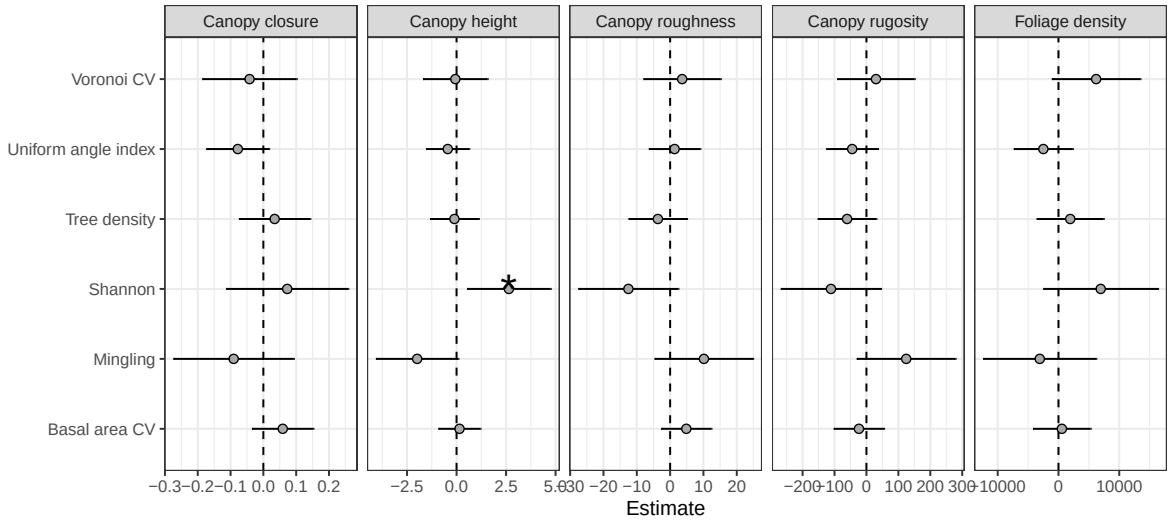

Figure 7: Standardised effect sizes for whole-plot canopy rugosity. Slope estimates where the interval (±1 standard error) does not overlap zero are considered to be significant effects, marked with asterisks.

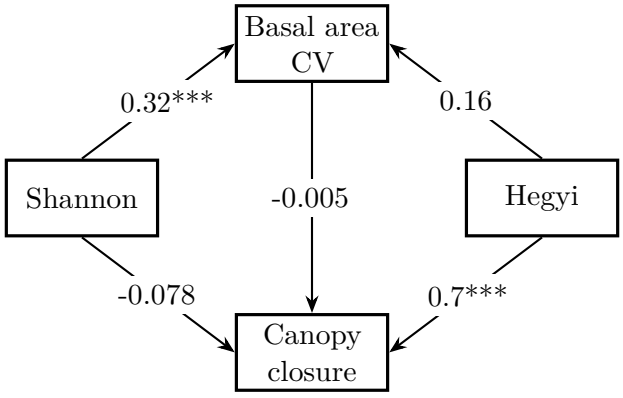

Figure 8: Directed Acyclic Graph showing standardised path coefficients of paths in the path analysis of the indirect effect of subplot species diversity (Shannon diversity index) on canopy closure via coefficient of variation of basal area. Asterisks define p-value thresholds: *<0.05, **<0.01, ***<0.001.

3.6 Comparing subplot and plot measures of canopy complexity

Plot and subplot canopy complexity metrics were highly correlated in many cases, with similar relationships among vegetation types (Figure 7). Most subplot and plot level canopy metrics covaried in a predictable manner. For example, increased canopy height led to an increase in canopy closure. Plot canopy height especially, tended to be strongly positively correlated with subplot canopy complexity metrics. Additionally, as canopy rugosity increased, many subplot canopy complexity and density metrics decreased. Subplot metrics varied greatly within plots, producing large uncertainty in plot level estimates of these metrics.

4 Discussion

This study investigated relationships between tree species diversity, stand structure, and several metrics of tree canopy complexity using terrestrial LiDAR in southern African savannas, with a view to improving understanding of the biotic drivers of variation in canopy complexity and vegetation dynamics. Species diversity appeared to generally have weak positive effects on canopy complexity metrics at both the subplot and plot scales. Plots with greater species diversity produced taller tree canopies, with a more complex within-canopy complexity, and greater canopy closure. However, inherent variability in canopy complexity among and within plots makes it difficult to conclusively infer a generalisable species diversity effect across all plots.

Plot level canopy complexity metrics were generally better predicted by species diversity and stand structure than subplot metrics. While positive relationships between species diversity and subplot canopy complexity metrics were observed in the subplot bivariate models, subplot linear mixed effects models did not show strong species diversity effects. Additionally, none of the best models for subplot canopy complexity metrics included species diversity as a fixed effect. This finding suggests a large degree of stochastic variability in canopy complexity within plots, that masks species effects at smaller spatial scales. The prevalence of disturbance events such as fire and damage by elephants in southern African woodlands, as well as tree-fall, small-scale variability in edaphic factors, and stochastic tree germination all contribute to heterogeneity in canopy complexity (). This study demonstrates the importance of large sample units and a high degree of replication when measuring canopy complexity, especially in disturbed systems, to effectively account for the inherent heterogeneity in the system ().

Spatial clustering of stems, measured using the uniform angle index, caused a clear decrease in canopy closure, with similar behaviour across vegetation types. Uniform angle index was also included in the best multivariate model predicting canopy closure. This finding is expected, as spatial clustering results in reduced canopy cover in areas outside clusters, and a non-compensatory increase in canopy closure within clusters, due to competition among individuals (). Clustering of trees in savannas can result from positive feedback effects from disturbance by fire and herbivory (). This study suggests that as well as reducing canopy cover, i.e. the ground area covered by tree canopies, disturbances in savannas may also serve to decrease canopy closure, i.e. the visible sky proportion from both within canopy gaps and between canopy gaps, indirectly by increasing spatial clustering of trees. The negative effects of spatial clustering on canopy closure are expected to increase in species poor woodlands, due to a lack of niche complementarity among coexisting individuals ().

Stand structural diversity caused positive canopy complexity effects for within-canopy structural metrics such as layer diversity and canopy surface roughness, but had negligible effects on canopy density. This is in line with other studies in forest ecosystems, which report that variation in tree size increases total canopy volume occupancy by increasing the number of canopy layers, but does not necessarily result in a concomitant increase in canopy closure, as the resulting canopies are often more sparse, especially for understorey individuals (). The path analysis

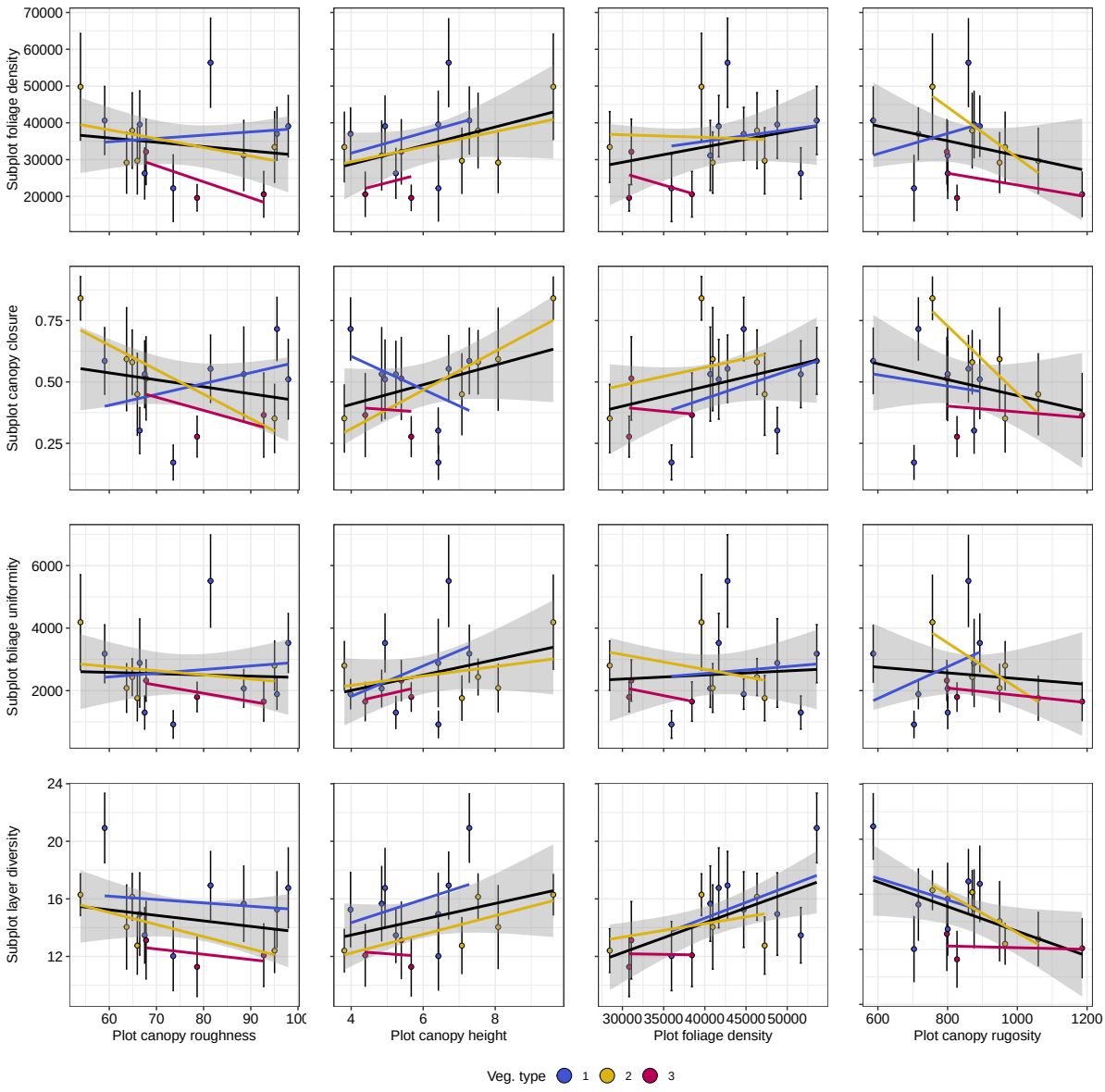

Figure 9: Bivariate plots comparing canopy structural metrics at the plot (x axis) and subplot scale (y axis). Each point represents the mean values of a single plot. Points and linear model fits are coloured according to vegetation type. The black linear model combines all vegetation types. Error bars on points are the standard deviation of mean subplot metrics across the plot. Note that because plot level canopy closure is calculated as the mean of subplot canopy closure, a comparison of subplot and plot canopy closure is not made in this figure.

also supports this conclusion, where species diversity was found to cause an increase in stand structural diversity, but this did not extend to an increase in canopy closure.

The effect of stand structure on canopy complexity in this system appears to be a result of demographic effects rather than variation in growth form as a function of species diversity. The path analysis testing the indirect effect of species diversity on canopy closure via stand structural diversity did not find a significant indirect effect of species diversity on canopy closure. While other studies in forests have found a species diversity effect on stand structural diversity (), it is suggested here that prevailing disturbance pressures mask any species diversity effect.

Effects of species composition, measured by vegetation type, on canopy complexity were small. While vegetation types differed in mean values for stand structural and species diversity metrics, variation in these metrics produced results of similar direction and magnitude among vegetation types in most cases. Small sample sizes for *Baikiaea* and ex-Acacia vegetation however, led to wide errors on most relationships especially at the plot level, such that it is impossible to draw deeper conclusions about the behaviour of these vegetation types. Variation in mean values of canopy complexity metrics among vegetation types is likely driven by species identity (), though species composition itself is likely driven by environmental factors and disturbance regime ().

Thoughts on the suitability of different canopy complexity metrics in sparse and clustered savannas. Lots of stochstic variation in stand structure

Lots of disturbance is exogenous, i.e. not controlled by stand composition, lots of noise

5 Conclusion

References

Archibald, S. & W. J. Bond (2003). 'Growing tall vs growing wide: tree architecture and allometry of Acacia karroo in forest, savanna, and arid environments'. In: *Oikos* 102.1, pp. 3–14. DOI: 10.1034/j.1600-0706.2003.12181.x.

Axelsson, C. R. & N. P. Hanan (2018). 'Rates of woody encroachment in African savannas reflect water constraints and fire disturbance'. In: *Journal of Biogeography* 45.6, pp. 1209–1218. DOI: 10.1111/jbi.13221.

Baldocchi, D. D. & K. B. Wilson (2001). 'Modeling CO2 and water vapor exchange of a temperate broadleaved forest across hourly to decadal time scales'. In: *Ecological Modelling* 142.1-2, pp. 155–184. DOI: 10.1016/s0304-3800(01)00287-3.

Barry, K. E., L. Mommer, J. van Ruijven, C. Wirth, A. J. Wright, Y. Bai, J. Connolly, G. B. D. Deyn, H. de Kroon, F. Isbell et al. (2019). 'The Future of Complementarity: Disentangling Causes from Consequences'. In: *Trends in Ecology & Evolution* 34.2, pp. 167–180. DOI: 10.1016/j.tree.2018.10.013.

Bond, W. J. & G. F. Midgley (2012). 'Carbon dioxide and the uneasy interactions of trees and savannah grasses'. In: *Philosophical Transactions of the Royal Society B: Biological Sciences* 367.1588, pp. 601–612. DOI: 10.1098/rstb.2011.0182.

Buitenwerf, R., W. J. Bond, N. Stevens & W. S. W. Trollope (2012). 'Increased tree densities in South African savannas: >50 years of data suggests CO_2 as a driver'. In: *Global Change Biology* 18.2, pp. 675–684. DOI: 10.1111/j.1365-2486.2011.02561.x.

Calders, K., J. Adams, J. Armston, H. Bartholomeus, S. Bauwens, L. P. Bentley, J. Chave, F. M. Danson, M. Demol, M. Disney et al. (2020). 'Terrestrial laser scanning in forest ecology: Expanding the horizon'. In: *Remote Sensing of Environment* 251, p. 112102. DOI: 10.1016/j.rse.2020.112102.

Charles-Dominique, T., G. F. Midgley, K. W. Tomlinson & W. J. Bond (2018). 'Steal the light: shade vs fire adapted vegetation in forest-savanna mosaics'. In: *New Phytologist* 218.4, pp. 1419–1429. DOI: 10.1111/nph.15117.

Chen, J. M., G. Mo, J. Pisek, J. Liu, F. Deng, M. Ishizawa & D. Chan (2012). 'Effects of foliage clumping on the estimation of global terrestrial gross primary productivity'. In: *Global Biogeochemical Cycles* 26, GB1019. DOI: 10.1029/2010gb003996.

Cifuentes, R., D. V. der Zande, J. Farifteh, C. Salas & P. Coppin (2014). 'Effects of voxel size and sampling setup on the estimation of forest canopy gap fraction from terrestrial laser scanning data'. In: *Agricultural and Forest Meteorology* 194, pp. 230–240. DOI: 10.1016/j.agrformet.2014.04.013.

Criado, M. G., I. H. Myers-Smith, A. D. Bjorkman, C. E. R. Lehmann & N. Stevens (2020). 'Woody plant encroachment intensifies under climate change across tundra and savanna biomes'. In: *Global Ecology and Biogeography* 29.5, pp. 925–943. DOI: 10.1111/geb.13072.

Dohn, J., D. J. Augustine, N. P. Hanan, J. Ratnam & M. Sankaran (2017). 'Spatial vegetation patterns and neighborhood competition among woody plants in an East African savanna'. In: *Ecology* 98.2, pp. 478–488. DOI: 10.1002/ecy.1659.

Donohue, R. J., M. L. Roderick, T. R. McVicar & G. D. Farquhar (2013). 'Impact of CO_2 fertilization on maximum foliage cover across the globe's warm, arid environments'. In: *Geophysical Research Letters* 40.12, pp. 3031–3035. DOI: 10.1002/grl.50563.

Ehbrecht, M., P. Schall, J. Juchheim, C. Ammer & D. Seidel (2016). 'Effective number of layers: A new measure for quantifying three-dimensional stand structure based on sampling with terrestrial LiDAR'. In: *Forest Ecology and Management* 380, pp. 212–223. DOI: 10.1016/j.foreco.2016.09.003.

Fotis, A. T., T. H. Morin, R. T. Fahey, B. S. Hardiman, G. Bohrer & P. S. Curtis (2018). 'Forest structure in space and time: Biotic and abiotic determinants of canopy complexity and their effects on net primary productivity'. In: *Agricultural and Forest Meteorology* 250-251, pp. 181–191. DOI: 10.1016/j.agrformet.2017.12.251.

Frost, P. (1996). 'The ecology of miombo woodlands'. In: *The miombo in transition: woodlands and welfare in Africa*. Ed. by B. Campbell. Bogor, Indonesia: Center for International Forestry Research, pp. 11–55.

Gough, C. M., J. W. Atkins, R. T. Fahey & B. S. Hardiman (2019). 'High rates of primary production in structurally complex forests'. In: *Ecology* 100.10. DOI: 10.1002/ecy.2864.

Hardiman, B. S., G. Bohrer, C. M. Gough, C. S. Vogel & P. S. Curtis (2011). 'The role of canopy structural complexity in wood net primary production of a maturing northern deciduous forest'. In: *Ecology* 92.9, pp. 1818–1827. DOI: 10.1890/10-2192.1.

Hegyi, F. (1974). 'A simulation model for managing jack-pine stands'. In: *Royal College of Forestry, editor*. Stockholm, Sweden: Royal College of Forestry, pp. 74–90.

Hirota, M., M. Holmgren, E. H. Van Nes & M. Scheffer (2011). 'Global resilience of tropical forest and savanna to critical transitions'. In: *Science* 334, pp. 232–235. DOI: 10.1126/science.1210657.

Jonckheere, I., S. Fleck, K. Nackaerts, B. Muys, P. Coppin, M. Weiss & F. Baret (2004). 'Review of methods for in situ leaf area index determination'. In: *Agricultural and Forest Meteorology* 121.1-2, pp. 19–35. DOI: 10.1016/j.agrformet.2003.08.027.

Jucker, T., O. Bouriaud & D. A. Coomes (2015). 'Crown plasticity enables trees to optimize canopy packing in mixed-species forests'. In: *Functional Ecology* 29.8, pp. 1078–1086. DOI: 10.1111/1365-2435.12428.

Kershaw, J. A., M. J. Ducey, T. W. Beers & B. Husch (2017). *Forest Mensuration*. Chichester, UK: John Wiley & Sons. ISBN: 9781118902035.

Khosravipour, A., A. K. Skidmore, M. Isenburg, T. Wang & Y. A. Hussin (2014). 'Generating Pit-free Canopy Height Models from Airborne LiDAR'. In: *Photogrammetric Engineering & Remote Sensing* 80.9, pp. 863–872. DOI: 10.14358/pers.80.9.863.

Körner, C. (2017). 'A matter of tree longevity'. In: *Science* 355.6321, pp. 130–131. DOI: 10.1126/science.aal2449.

Law, B. E., A. Cescatti & D. D. Baldocchi (2001). 'Leaf area distribution and radiative transfer in open-canopy forests: implications for mass and energy exchange'. In: *Tree Physiology* 21.12-13, pp. 777–787. DOI: 10.1093/treephys/21.12-13.777.

Lefcheck, J. S. (2016). 'piecewiseSEM: Piecewise structural equation modeling in R for ecology, evolution, and systematics'. In: *Methods in Ecology and Evolution* 7.5, pp. 573–579. DOI: 10.1111/2041-210X.12512.

Lowman, M. D. & H. B. Rinker (2004). *Forest Canopies*. Physiological Ecology. Burlington MA, USA: Elsevier Science. ISBN: 9780080491349.

Mitchard, E. T. A. & C. M. Flintrop (2013). 'Woody encroachment and forest degradation in sub-Saharan Africa's woodlands and savannas 1982-2006'. In: *Philosophical Transactions of the Royal Society B: Biological Sciences* 368.1625, p. 20120406. DOI: 10.1098/rstb.2012.0406.

Morin, X. (2015). 'Species richness promotes canopy packing: a promising step towards a better understanding of the mechanisms driving the diversity effects on forest functioning'. In: *Functional Ecology* 29.8, pp. 993–994. DOI: 10.1111/1365-2435.12473.

Mugasha, W. A., O. M. Bollandsås & T. Eid (2013). 'Relationships between diameter and height of trees in natural tropical forest in Tanzania'. In: *Southern Forests: a Journal of Forest Science* 75.4, pp. 221–237. DOI: 10.2989/20702620.2013.824672.

Muir, J., S. Phinn, T. Eyre & P. Scarth (2018). 'Measuring plot scale woodland structure using terrestrial laser scanning'. In: *Remote Sensing in Ecology and Conservation* 4.4, pp. 320–338. DOI: 10.1002/rse2.82.

Muumbe, T. P., J. Baade, J. Singh, C. Schmullius & C. Thau (2021). 'Terrestrial Laser Scanning for Vegetation Analyses with a Special Focus on Savannas'. In: *Remote Sensing* 13.3, p. 507. DOI: 10.3390/rs13030507.

Nakagawa, S. & I. C. Cuthill (2007). 'Effect size, confidence interval and statistical significance: a practical guide for biologists'. In: *Biological Reviews* 82.4, pp. 591–605. DOI: 10.1111/j.1469-185x.2007.00027.x.

Ong, M. S., Y. C. Kuang & M. P.-L. Ooi (2012). 'Statistical measures of two dimensional point set uniformity'. In: *Computational Statistics & Data Analysis* 56.6, pp. 2159–2181. DOI: 10.1016/j.csda.2011.12.005.

Panzou, G. J. L., A. Fayolle, T. Jucker, O. L. Phillips, S. Bohlman, L. F. Banin, S. L. Lewis, K. Affum-Baffoe, L. F. Alves, C. Antin et al. (2020). 'Pantropical variability in tree crown allometry'. In: *Global Ecology and Biogeography* 30.2, pp. 459–475. DOI: 10.1111/geb.13231.

Persistence of Vision Pty. Ltd. (2004). *Persistence of Vision Raytracer (Version 3.7)*. [Computer software].

Pretzsch, H. (2014). 'Canopy space filling and tree crown morphology in mixed-species stands compared with monocultures'. In: *Forest Ecology and Management* 327, pp. 251–264. DOI: http://dx.doi.org/10.1016/j.foreco.2014.04.027.

Privette, J., Y. Tian, G. Roberts, R. Scholes, Y. Wang, K. Caylor, P. Frost & M. Mukelabai (2004). 'Vegetation structure characteristics and relationships of Kalahari woodlands and savannas'. In: *Global Change Biology* 10.3, pp. 281–291. DOI: 10.1111/j.1365-2486.2004.00740.x.

Ratcliffe, S., C. Wirth, T. Jucker, F. van der Plas, M. Scherer-Lorenzen, K. Verheyen, E. Allan, R. Benavides, H. Bruelheide, B. Ohse et al. (2017). 'Biodiversity and ecosystem functioning relations in European forests depend on environmental context'. In: *Ecology Letters* 20, pp. 1414–1426. DOI: http://dx.doi.org/10.1111/ele.12849.

Reich, P. B., S. E. Hobbie & T. D. Lee (2014). 'Plant growth enhancement by elevated CO2 eliminated by joint water and nitrogen limitation'. In: *Nature Geoscience* 7.12, pp. 920–924. DOI: 10.1038/ngeo2284.

Ribeiro, N. S., P. L. Silva de Miranda & J. Timberlake (2020). 'Biogeography and Ecology of Miombo Woodlands'. In: *Miombo Woodlands in a Changing Environment: Securing the*

Resilience and Sustainability of People and Woodlands. Ed. by N. S. Ribeiro, Y. Katerere, P. W. Chirwa & I. M. Grundy. Springer International Publishing, pp. 9–53. DOI: 10.1007/978-3-030-50104-4_2.

Rusu, R. B., Z. C. Marton, N. Blodow, M. Dolha & M. Beetz (2008). 'Towards 3D Point cloud based object maps for household environments'. In: *Robotics and Autonomous Systems* 56.11, pp. 927–941. DOI: 10.1016/j.robot.2008.08.005.

Sankaran, M., N. P. Hanan, R. J. Scholes, J. Ratnam, D. J. Augustine, B. S. Cade, J. Gignoux, S. I. Higgins, X. Le Roux, F. Ludwig et al. (2005). 'Determinants of woody cover in African savannas'. In: *Nature* 438.8, pp. 846–849. DOI: http://dx.doi.org/10.1038/nature04070.

Scheuermann, C. M., L. E. Nave, R. T. Fahey, K. J. Nadelhoffer & C. M. Gough (2018). 'Effects of canopy structure and species diversity on primary production in upper Great Lakes forests'. In: *Oecologia* 188.2, pp. 405–415. DOI: 10.1007/s00442-018-4236-x.

Scholes, R. J. & S. R. Archer (1997). 'Tree grass interactions in savannas'. In: *Annual Review of Ecology and Systematics*.

Seidel, D., S. Fleck & C. Leuschner (2012). 'Analyzing forest canopies with ground-based laser scanning: A comparison with hemispherical photography'. In: *Agricultural and Forest Meteorology* 154-155, pp. 1–8. DOI: 10.1016/j.agrformet.2011.10.006.

Seidel, D., S. Fleck, C. Leuschner & T. Hammett (2011). 'Review of ground-based methods to measure the distribution of biomass in forest canopies'. In: *Annals of Forest Science* 68.2, pp. 225–244. DOI: 10.1007/s13595-011-0040-z.

Shenkin, A., L. P. Bentley, I. Oliveras, N. Salinas, S. Adu-Bredu, B. H. Marimon-Junior, B. S. Marimon, T. Peprah, E. L. Choque, L. T. Rodriguez et al. (2020). 'The Influence of Ecosystem and Phylogeny on Tropical Tree Crown Size and Shape'. In: *Frontiers in Forests and Global Change* 3. DOI: 10.3389/ffgc.2020.501757. URL: https://doi.org/10.3389%2Fffgc.2020.501757.

Sitch, S., P. Friedlingstein, N. Gruber, S. D. Jones, G. Murray-Tortarolo, A. Ahlström, S. C. Doney, H. Graven, C. Heinze, C. Huntingford et al. (2015). 'Recent trends and drivers of regional sources and sinks of carbon dioxide'. In: *Biogeosciences* 12.3, pp. 653–679. DOI: 10.5194/bg-12-653-2015.

Solbrig, O. T., E. Medina & J. F. Silva (1996). *Biodiversity and Savanna Ecosystem Processes*. Berlin, Germany: Springer-Verlag.

Stark, S. C., B. J. Enquist, S. R. Saleska, V. Leitold, J. Schietti, M. Longo, L. F. Alves, P. B. Camargo & R. C. Oliveira (2015). 'Linking canopy leaf area and light environments with tree size distributions to explain Amazon forest demography'. In: *Ecology Letters* 18.7, pp. 636–645. DOI: 10.1111/ele.12440.

Staver, A. C. & S. E. Koerner (2015). 'Top-down and bottom-up interactions determine tree and herbaceous layer dynamics in savanna grasslands'. In: *Trophic Ecology: Bottom-up and Top-Down Interactions Across Aquatic and Terrestrial Systems*. Ed. by K. J. La Pierre & T. C. Hanley. Cambridge, United Kingdom: Cambridge University Press, pp. 86–106.

Stevens, N., C. E. R. Lehmann, B. P. Murphy & G. Durigan (2016). 'Savanna woody encroachment is widespread across three continents'. In: *Global Change Biology* 23.1, pp. 235–244. DOI: 10.1111/gcb.13409.

ter Steege, H. (2018). *Hemiphot.R: Free R scripts to analyse hemispherical photographs for canopy openness, leaf area index and photosynthetic active radiation under forest canopies*. Unpublished report. Leiden, The Netherlands: Naturalis Biodiversity Center. URL: https://github.com/Naturalis/Hemiphot.

von Gadow, K. & G. Hui (2002). *Characterising forest spatial structure and diversity*. Ed. by L. Bjoerk. Lund, Sweden, pp. 20–30.

White, F. (1983). *The Vegetation of Africa: A descriptive memoir to accompany the UNESCO/AETFAT/UNSO vegetation map of Africa*. Paris, France: UNESCO. DOI: 10.2307/2260340.

Wright, A. J., W. D. A. Wardle, W. R. Callaway & A. Gaxiola (2017). 'The overlooked role of facilitation in biodiversity experiments'. In: *Trends in Ecology & Evolution* 32, pp. 383–390. DOI: 10.1016/j.tree.2017.02.011.

Zhang, K., S.-C. Chen, D. Whitman, M.-L. Shyu, J. Yan & C. Zhang (2003). 'A progressive morphological filter for removing nonground measurements from airborne LIDAR data'. In: *IEEE Transactions on Geoscience and Remote Sensing* 41.4, pp. 872–882. DOI: 10.1109/tgrs.2003.810682.

Table 6: Summary statistics of bivariate linear models comparing canopy complexity metrics with diversity and stand structural metrics. Slope refers to the slope of the predictor term in the model, ± 1 standard error. T is the t-value of the slope of the predictor term in the model, Asterisks indicate the p-value of these terms (***<0.001, **<0.01, *<0.05).

Response	Predictor	Cluster	Slope	F	R^2	T
Foliage density	Basal area CV	1	7.3e+01±3.7e+01	4.0(2,97)	0.04	1.99*
		2	1.1e+02±7.9e+01	2.1(2,38)	0.05	1.44
		3	1.4e+01±7.2e+01	0.0(2,14)	0.00	0.20
		4	1.6e+01±2.0e+02	0.0(2,12)	0.00	0.08
Foliage density	Hegyi	1	5.9e+03±2.1e+03	8.2(2,102)	0.07	2.86**
		2	1.4e+04±3.6e+03	15.2(2,40)	0.28	3.90***
		3	6.6e+03±3.0e+03	4.8(2,23)	0.17	2.18*
		4	1.5e+01±5.5e+03	0.0(2,13)	0.00	0.00
Foliage density	Shannon	1	2.2e+03±1.3e+03	2.8(2,102)	0.03	1.67
		2	3.8e+03±2.4e+03	2.6(2,39)	0.06	1.61
		3	1.1e+04±6.5e+03	3.1(2,20)	0.13	1.77
		4	-6.5e+03±6.5e+03	1.0(2,13)	0.07	−1.01
Canopy closure	Basal area CV	1	1.7e-04±6.0e-04	0.1(2,97)	0.00	0.28
		2	2.9e-03±1.1e-03	6.9(2,39)	0.15	2.62*
		3	4.2e-03±1.1e-03	15.1(2,14)	0.52	3.89**
		4	-4.6e-03±3.0e-03	2.2(2,12)	0.16	−1.50
Canopy closure	Hegyi	1	2.2e-01±2.8e-02	62.3(2,102)	0.38	7.89***
		2	2.6e-01±5.1e-02	27.0(2,41)	0.40	5.19***
		3	2.8e-01±4.0e-02	50.7(2,23)	0.69	7.12***
		4	1.7e-01±8.0e-02	4.5(2,13)	0.26	2.12
Canopy closure	Shannon	1	3.1e-03±2.2e-02	0.0(2,102)	0.00	0.14
		2	1.1e-01±3.2e-02	12.1(2,40)	0.23	3.48**
		3	2.3e-01±1.4e-01	2.9(2,20)	0.13	1.69
		4	6.7e-02±1.1e-01	0.4(2,13)	0.03	0.60
Foliage uniformity	Basal area CV	1	3.7e+00±4.0e+00	0.9(2,97)	0.01	0.92
		2	4.5e+00±7.4e+00	0.4(2,38)	0.01	0.61
		3	-3.5e+00±5.9e+00	0.4(2,14)	0.02	−0.59
		4	-9.3e-01±1.5e+01	0.0(2,12)	0.00	−0.06
Foliage uniformity	Hegyi	1	2.2e+02±2.3e+02	1.0(2,102)	0.01	0.98
		2	7.5e+02±3.7e+02	4.0(2,40)	0.09	2.00
		3	4.5e+02±2.6e+02	2.9(2,23)	0.11	1.72
		4	-7.5e+01±4.0e+02	0.0(2,13)	0.00	−0.19
Foliage uniformity	Shannon	1	2.3e+02±1.4e+02	2.6(2,102)	0.02	1.61

		2	8.6e+01±2.2e+02	0.1(2,39)	0.00	0.38
		3	1.3e+03±5.1e+02	6.1(2,20)	0.23	2.48*
		4	-5.9e+02±4.7e+02	1.6(2,13)	0.11	−1.27
Layer diversity	Basal area CV	1	2.5e-02±9.3e-03	7.1(2,97)	0.07	2.66**
		2	3.9e-02±1.4e-02	8.0(2,38)	0.17	2.83**
		3	2.7e-02±2.3e-02	1.3(2,14)	0.09	1.15
		4	2.1e-02±3.1e-02	0.5(2,12)	0.04	0.67
Layer diversity	Hegyi	1	2.7e+00±4.9e-01	29.1(2,102)	0.22	5.39***
		2	2.0e+00±7.5e-01	7.1(2,40)	0.15	2.66*
		3	1.9e+00±1.0e+00	3.6(2,23)	0.13	1.89
		4	1.1e+00±8.5e-01	1.8(2,13)	0.12	1.33
Layer diversity	Shannon	1	1.0e+00±3.4e-01	8.7(2,102)	0.08	2.95**
		2	9.5e-01±4.3e-01	4.8(2,39)	0.11	2.18*
		3	4.9e+00±1.8e+00	7.2(2,20)	0.26	2.68*
		4	1.8e-01±1.1e+00	0.0(2,13)	0.00	0.16
Canopy roughness	Basal area CV	1	1.2e-01±6.9e-02	2.9(2,6)	0.33	1.72
		2	-3.2e-01±2.9e-01	1.2(2,3)	0.29	−1.10
		3	3.5e-01±4.7e-01	0.6(2,1)	0.36	0.74
		4				
Canopy roughness	Voronoi CV	1	2.6e-01±1.2e+00	0.0(2,6)	0.01	0.22
		2	4.6e+00±1.9e+00	6.1(2,3)	0.67	2.48
		3	1.8e+00±1.9e+00	1.0(2,1)	0.49	0.99
		4				
Canopy roughness	Mingling	1	-4.2e+01±5.7e+01	0.5(2,6)	0.08	−0.74
		2	1.6e+01±9.7e+01	0.0(2,3)	0.01	0.17
		3	3.5e+02±2.5e+02	2.0(2,1)	0.67	1.42
		4				
Canopy roughness	Tree density	1	-4.3e-02±4.5e-02	0.9(2,6)	0.13	−0.96
		2	-5.9e-02±3.1e-02	3.6(2,3)	0.54	−1.89
		3	-1.8e-01±2.6e-01	0.5(2,1)	0.31	−0.68
		4				
Canopy roughness	Shannon	1	-2.3e+00±1.7e+00	1.7(2,6)	0.22	−1.32
		2	-1.4e+00±2.4e+00	0.4(2,3)	0.11	−0.60
		3	3.4e+01±4.7e+01	0.5(2,1)	0.34	0.72
		4				
Canopy roughness	Uniform angle index	1	-7.4e+01±2.6e+02	0.1(2,6)	0.01	−0.28
		2	4.1e+02±9.5e+02	0.2(2,3)	0.06	0.43
		3	4.4e+02±5.7e+02	0.6(2,1)	0.37	0.76
		4				
Canopy height	Basal area CV	1	-6.5e-03±6.1e-03	1.1(2,6)	0.16	−1.07
		2	4.3e-02±4.0e-02	1.2(2,3)	0.28	1.08
		3	-3.1e-02±8.7e-03	12.3(2,1)	0.92	−3.51
		4				
Canopy height	Voronoi CV	1	-1.0e-01±8.6e-02	1.5(2,6)	0.20	−1.21
		2	-7.0e-01±2.0e-01	12.7(2,3)	0.81	−3.57*
		3	-1.8e-02±1.4e-01	0.0(2,1)	0.02	−0.13

		4				
Canopy height	Mingling	1 2 3 4	6.8e+00±3.8e+00 -3.3e+00±1.3e+01 -2.3e+01±9.3e-01	3.2(2,6) 0.1(2,3) 619.2(2,1)	0.34 0.02 1.00	1.78 −0.25 −24.88*
Canopy height	Tree density	1 2 3 4	-3.5e-04±3.8e-03 8.6e-03±4.0e-03 -1.0e-03±1.7e-02	0.0(2,6) 4.7(2,3) 0.0(2,1)	0.00 0.61 0.00	−0.09 2.16 −0.06
Canopy height	Shannon	1 2 3 4	2.8e-01±1.1e-01 1.7e-01±3.3e-01 -3.0e+00±9.0e-01	7.1(2,6) 0.3(2,3) 11.1(2,1)	0.54 0.08 0.92	2.66* 0.52 −3.32
Canopy height	Uniform angle index	1 2 3 4	1.0e+01±2.1e+01 -7.2e+01±1.3e+02 6.0e-02±3.9e+01	0.2(2,6) 0.3(2,3) 0.0(2,1)	0.04 0.09 0.00	0.49 −0.56 0.00
Canopy closure	Basal area CV	1 2 3 4	3.6e-04±6.9e-04 3.5e-03±3.5e-03 1.9e-03±5.3e-03	0.3(2,10) 1.0(2,3) 0.1(2,1)	0.03 0.24 0.11	0.53 0.98 0.35
Canopy closure	Voronoi CV	1 2 3 4	9.3e-03±8.2e-03 -6.6e-02±7.9e-03 -2.5e-02±4.6e-03	1.3(2,10) 69.7(2,3) 29.0(2,1)	0.11 0.96 0.97	1.13 −8.35** −5.39
Canopy closure	Mingling	1 2 3 4	-1.6e-01±5.1e-01 -6.9e-01±1.1e+00 7.6e-02±4.1e+00	0.1(2,10) 0.4(2,3) 0.0(2,1)	0.01 0.12 0.00	−0.31 −0.63 0.02
Canopy closure	Tree density	1 2 3 4	1.4e-04±4.0e-04 8.5e-04±2.4e-04 3.0e-03±4.3e-06	0.1(2,10) 12.2(2,3) 499683.9(2,1)	0.01 0.80 1.00	0.36 3.50* 706.88***
Canopy closure	Shannon	1 2 3 4	-7.6e-03±1.7e-02 8.5e-03±3.0e-02 1.9e-01±5.2e-01	0.2(2,10) 0.1(2,3) 0.1(2,1)	0.02 0.03 0.12	−0.45 0.28 0.37
Canopy closure	Uniform angle index	1 2 3 4	-3.9e+00±2.3e+00 -1.2e+01±9.3e+00 -6.9e+00±3.9e-01	2.9(2,10) 1.7(2,3) 306.2(2,1)	0.23 0.36 1.00	−1.71 −1.30 −17.50*
Foliage density	Basal area CV	1 2 3 4	-4.5e+01±2.9e+01 1.5e+02±1.4e+02 1.8e+02±8.9e+01	2.3(2,6) 1.1(2,3) 4.2(2,1)	0.28 0.27 0.81	−1.52 1.05 2.06
Foliage density	Voronoi CV	1	3.5e+01±5.0e+02	0.0(2,6)	0.00	0.07

		2	-7.7e+02±1.5e+03	0.3(2,3)	0.08	−0.51
		3	2.7e+02±8.7e+02	0.1(2,1)	0.09	0.31
		4				
Foliage density	Mingling	1	4.5e+03±2.5e+04	0.0(2,6)	0.01	0.18
		2	8.0e+02±4.7e+04	0.0(2,3)	0.00	0.02
		3	1.5e+05±2.0e+04	54.1(2,1)	0.98	7.35
		4				
Foliage density	Tree density	1	8.8e+00±2.0e+01	0.2(2,6)	0.03	0.45
		2	1.1e+01±2.1e+01	0.3(2,3)	0.08	0.51
		3	-1.3e+01±1.1e+02	0.0(2,1)	0.01	−0.12
		4				
Foliage density	Shannon	1	2.5e+02±8.1e+02	0.1(2,6)	0.02	0.31
		2	5.0e+02±1.2e+03	0.2(2,3)	0.05	0.42
		3	1.8e+04±9.1e+03	3.9(2,1)	0.80	1.98
		4				
Foliage density	Uniform angle index	1	-1.1e+05±1.0e+05	1.3(2,6)	0.18	−1.15
		2	1.2e+05±4.7e+05	0.1(2,3)	0.02	0.25
		3	4.3e+04±2.5e+05	0.0(2,1)	0.03	0.18
		4				
Canopy rugosity	Basal area CV	1	-1.0e-01±6.1e-01	0.0(2,6)	0.00	−0.17
		2	-2.2e+00±2.2e+00	1.1(2,3)	0.26	−1.03
		3	8.7e+00±5.4e+00	2.6(2,1)	0.73	1.62
		4				
Canopy rugosity	Voronoi CV	1	7.9e+00±8.2e+00	0.9(2,6)	0.13	0.96
		2	3.5e+01±1.3e+01	6.8(2,3)	0.69	2.61
		3	1.8e+01±4.2e+01	0.2(2,1)	0.15	0.42
		4				
Canopy rugosity	Mingling	1	-5.9e+02±3.6e+02	2.7(2,6)	0.31	−1.63
		2	8.5e+02±5.2e+02	2.7(2,3)	0.47	1.63
		3	7.2e+03±1.7e+03	17.6(2,1)	0.95	4.19
		4				
Canopy rugosity	Tree density	1	-1.9e-01±3.4e-01	0.3(2,6)	0.05	−0.56
		2	-4.6e-01±2.1e-01	4.9(2,3)	0.62	−2.22
		3	-1.2e+00±5.4e+00	0.0(2,1)	0.05	−0.22
		4				
Canopy rugosity	Shannon	1	-2.4e+01±1.0e+01	5.3(2,6)	0.47	−2.31
		2	6.4e+00±1.8e+01	0.1(2,3)	0.04	0.35
		3	8.5e+02±5.4e+02	2.5(2,1)	0.71	1.57
		4				
Canopy rugosity	Uniform angle index	1	-2.6e+03±1.6e+03	2.5(2,6)	0.30	−1.58
		2	1.0e+04±4.1e+03	6.1(2,3)	0.67	2.47
		3	3.4e+03±1.2e+04	0.1(2,1)	0.07	0.28
		4				

Table 3: Summary statistics of bivariate linear models comparing canopy complexity metrics with diversity and stand structural metrics across all vegetation types. Slope refers to the slope of the predictor term in the model, ± 1 standard error. T is the t-value of the slope of the predictor term in the model, Asterisks indicate the p-value of these terms (***<0.001, **<0.01, *<0.05).

Response	Predictor	Slope	F	R^2	T
Foliage density	Basal area CV	8.7e+01±3.0e+01	8.6(2,167)	0.05	2.93**
	Hegyi	7.8e+03±1.6e+03	25.5(2,184)	0.12	5.05***
	Shannon	3.2e+03±1.1e+03	8.9(2,180)	0.05	2.98**
Canopy closure	Basal area CV	1.2e-03±4.8e-04	6.3(2,168)	0.04	2.52*
	Hegyi	2.4e-01±2.1e-02	132.8(2,185)	0.42	11.52***
	Shannon	4.7e-02±1.7e-02	7.3(2,181)	0.04	2.70**
Foliage uniformity	Basal area CV	4.1e+00±3.0e+00	1.9(2,167)	0.01	1.37
	Hegyi	4.0e+02±1.6e+02	6.2(2,184)	0.03	2.49*
	Shannon	2.2e+02±1.1e+02	4.1(2,180)	0.02	2.04*
Layer diversity	Basal area CV	3.2e-02±7.6e-03	17.6(2,167)	0.10	4.20***
	Hegyi	2.7e+00±3.9e-01	46.8(2,184)	0.20	6.84***
	Shannon	1.1e+00±2.7e-01	16.8(2,180)	0.09	4.10***
Canopy roughness	Basal area CV	3.0e-02±5.0e-02	0.4(2,16)	0.02	0.60
	Voronoi CV	7.5e-01±5.9e-01	1.6(2,16)	0.09	1.26
	Mingling	-2.8e+01±3.3e+01	0.7(2,16)	0.04	−0.86
	Tree density	-2.6e-02±1.7e-02	2.3(2,16)	0.12	−1.51
	Shannon	-1.9e+00±9.5e-01	4.0(2,16)	0.20	−2.01
	Uniform angle index	1.6e+02±1.6e+02	1.0(2,16)	0.06	0.98
Canopy height	Basal area CV	7.1e-03±7.3e-03	0.9(2,16)	0.06	0.97
	Voronoi CV	-4.7e-02±9.1e-02	0.3(2,16)	0.02	−0.52
	Mingling	3.8e+00±4.8e+00	0.6(2,16)	0.04	0.79
	Tree density	4.3e-03±2.5e-03	3.1(2,16)	0.16	1.76
	Shannon	3.3e-01±1.3e-01	6.0(2,16)	0.27	2.45*
	Uniform angle index	-2.2e+01±2.4e+01	0.8(2,16)	0.05	−0.90
Canopy closure	Basal area CV	8.5e-04±5.7e-04	2.2(2,20)	0.10	1.50
	Voronoi CV	2.4e-03±5.8e-03	0.2(2,20)	0.01	0.41
	Mingling	7.2e-03±3.7e-01	0.0(2,20)	0.00	0.02
	Tree density	4.7e-04±1.9e-04	6.3(2,20)	0.24	2.50*
	Shannon	1.0e-02±1.2e-02	0.7(2,20)	0.04	0.86
	Uniform angle index	-3.4e+00±1.7e+00	3.9(2,20)	0.16	−1.98
Foliage density	Basal area CV	5.8e+01±3.2e+01	3.3(2,16)	0.17	1.80
	Voronoi CV	5.8e+02±4.1e+02	2.1(2,16)	0.11	1.43
	Mingling	6.6e+03±2.3e+04	0.1(2,16)	0.01	0.29
	Tree density	3.0e+01±1.0e+01	8.6(2,16)	0.35	2.93**
	Shannon	1.1e+03±6.9e+02	2.5(2,16)	0.13	1.57
	Uniform angle index	-2.1e+04±1.1e+05	0.0(2,16)	0.00	−0.18
Canopy rugosity	Basal area CV	-1.0e+00±5.3e-01	3.7(2,16)	0.19	−1.92
	Voronoi CV	-6.0e+00±7.0e+00	0.7(2,16)	0.04	−0.86
	Mingling	1.3e+02±3.8e+02	0.1(2,16)	0.01	0.33
	Tree density	-5.2e-01±1.7e-01	10.0(2,16)	0.38	−3.16**
	Shannon	-1.3e+01±1.2e+01	1.2(2,16)	0.07	−1.11
	Uniform angle index	-1.8e+03±1.9e+03	0.9(2,16)	0.06	−0.97

Table 4: Explanatory variables included in the best model for each canopy structure variable. ΔAIC shows the difference in model AIC value compared to a null model which included only the random effects of vegetation type and plot. Positive ΔAIC values indicate that the model is of better quality than the null model. R^2_c is the R^2 of the best model, while R^2_m is the R^2 of the model fixed effects only.

Response	Hegyi	Shannon	Basal area CV	ΔAIC	R^2_c	R^2_m
Layer diversity	✓		✓	37.0	0.50	0.17
Foliage density	✓			62.3	0.27	0.09
Foliage uniformity	✓			33.1	0.29	0.02
Canopy closure	✓			93.9	0.60	0.46

Table 5: Explanatory variables included in the best linear model for each plot-level canopy complexity metric. ΔAIC shows the difference in model AIC value compared to a null model. Positive ΔAIC values indicate that the model is of better quality than the null model.

Response	Shannon	Tree density	Basal area CV	Mingling	Uniform angle index	Voronoi CV	ΔAIC	R^2	Prob.
Foliage density		✓					3.8	0.58	0.08
Canopy closure			✓		✓		1.9	0.54	0.13
Canopy height	✓			✓			2.1	0.54	0.12
Canopy roughness	✓						0.3	0.50	0.19
Canopy rugosity		✓					4.0	0.59	0.08